# Preparation, structural evaluation and adsorptive properties of activated carbon from agricultural waste biomass

**Article** *in* Advanced Powder Technology · February 2015

DOI: 10.1016/j.apt.2015.02.006



**2 authors:**

Eda Koseoglu
Koc University
**3** PUBLICATIONS **346** CITATIONS

SEE PROFILE

Canan Akmil-Başar
Inonu University
**35** PUBLICATIONS **1,867** CITATIONS

SEE PROFILE

Advanced Powder Technology 26 (2015) 811–818

Contents lists available at ScienceDirect

Advanced Powder Technology

journal homepage: www.elsevier.com/locate/apt

Original Research Paper

# Preparation, structural evaluation and adsorptive properties of activated carbon from agricultural waste biomass

Eda Köseoğlu, Canan Akmil-Başar *

*Department of Chemical Engineering, Faculty of Engineering, Inonu University, 44280 Malatya, Turkey*

ARTICLE INFO

*Article history:*
Received 27 October 2014
Received in revised form 16 January 2015
Accepted 10 February 2015
Available online 28 February 2015

*Keywords:*
Activated carbon
Waste
Orange peel
Chemical activation

ABSTRACT

The purpose of this study is to produce the low-cost activated carbon from the orange peel, known as a waste of fruit juice industry, by chemical activation using zinc chloride ($ZnCl_2$) and potassium carbonate ($K_2CO_3$). The effects of the activation temperature and type of activation reagents on the surface and chemical properties of activated carbon were investigated. The activation temperatures and impregnation ratios were selected at the range of 500–1000 °C and 1:1, respectively. The carbon content of activated carbons resulted 70% while BET surface area of activated carbons prepared with $K_2CO_3$ and $ZnCl_2$ activation is 1352 $m^2 g^{-1}$ and 1215 $m^2 g^{-1}$ respectively. An increase in the temperature for both $K_2CO_3$ and $ZnCl_2$ led to a decrease in the yields of the activated carbons. The yield of $ZnCl_2$ series is higher than that of $K_2CO_3$. The obtained activated carbons were heterosporous with the micropore.


## 1. Introduction

Activated carbon (AC) obtained from agricultural by-products has the some advantage like efficiency and low cost If they are compared with non-renewable coal-based granular activated carbons [1]. The abundance and availability of agricultural by-products makes them good sources of raw materials for activated carbon production [2]. In recent years, this has promoted a growing research interest in the use of alternative waste materials from industry and agriculture for activated carbon production [3–5]. One of the main challenges in the commercial manufacture of activated carbons is to identify new precursors that are cheap, therefore, a lot of research has been reported on activated carbons from agricultural wastes, including corn cob [6], coconut shell [7], palm shell [8], apple pulp [9], chickpea husks [10], grain sorghum [11], pistachio nut shell [12], jute fiber [13], olive stones and walnut shell [14], cherry stones [15], coir pith [16], wild rose seeds [17], rice bran [18], gopher plant [19], jackfruit shell waste [4], oil palm shell [20], rubber tree seed coat [21], cotton stalk [22], flamboyant [23], beach casuarina, lantana weed, tea waste, sugarcane bagasse and empty oil palm fruit bunches [24]. Palmyra tree leaves, inflorescence and fruit nutshell waste [25] have been found to be suitable precursors owing to their high carbon and low ash contents [26–31]. Chemical activation of AC has been reported as more advantageous over physical activation due to higher yields, more surface area and better development of porous structures in carbon [32–35]. According to the Food and Agriculture Organization (FAO), the annual production of orange fruit in 2010 is projected at 66.4 million tonnes, translating to approximately 32 million tonnes of peels as the byproducts [36].

Traditionally, orange peel (OP) were processed to obtain the volatile and nonvolatile fractions of essential oils and flavoring in the carbonated drinks, ice creams, cakes, air-fresheners, perfumes and cosmetic products [37]. Besides, OP have been reported to have germicidal, antioxidant and anti-carcinogenic properties as a remedy against breast and colon cancer, stomach upset, skin inflammation, muscle pain, and ringworm infections [38]. However, the application of these extracted constituents is limited due the overall demands for these value-added products are relatively insignificant. Therefore, it is necessary to find a rapid and easy route toward upgrading of the citrus processing biomass.

Thus the object of the present research work has been to explore an economically viable carbon precursor for the production of activated carbon materials. To our knowledge, this is the first time that the production of activated carbon are provided by chemical activation with $ZnCl_2$ and $K_2CO_3$

## 2. Materials and methods

### 2.1. Preparation activated carbon

Orange peel (OP), outer skin with white inner skin, a by-product collected from the local restaurant and fruit juice industries, was

* Corresponding author. Tel.: +90 422 3774734; fax: +90 422 341 00 46.
*E-mail address:* canan.basar@inonu.edu.tr (C. Akmil-Başar).

http://dx.doi.org/10.1016/j.apt.2015.02.006
0921-8831/

the precursor used in the present study. The raw precursor was washed exhaustively with deionized water to remove adhering dirt particles from the surface. Dried (at 110 °C) OP was cut, sized to a particle size of 4 mm. The results of proximate and ultimate analysis of orange peel are given in Table 1.

In the first step of activation, the starting material was mixed with $ZnCl_2$ at the $ZnCl_2$/starting material weight ratio of 1:1 and the mixture was knead with adding distilled water. The mixture was then dried at 110 °C to prepare the impregnated sample. In the second step, the impregnated sample was placed on a quartz dish, which was then inserted in a quartz tube (inlet diameter 60 mm). The same method and ratio also is applied for $K_2CO_3$.

Carbonization of the impregnated samples was carried out in a 316 stainless steel tubular reactor (Protherm PTF 12, Fig. 1) with a length of 90 mm and an internal diameter of 105 mm under nitrogen flow. The impregnated sample was heated up to activation temperature under $N_2$ flow (100 ml $min^{-1}$) at heating rate of 10 °C $min^{-1}$ and held for 1 h at this activation temperature. The activation temperature varied from 400 to 1000 °C (samples are coded OPZn4, OPZn5, OPZn6, OPZn7, OPZn8, and OPZn9). Adsorbents (OPKC5, OPKC7, OPKC8, OPKC9, OPKC95, and OPKC10) were prepared from orange peels by chemical activation with $K_2CO_3$. After activation, the sample was cooled down under $N_2$ flow and 0.5 N HCl was added on to OPZn activated samples. HCl were not added on to OPKC activated carbons. The activated carbons were further washed with distillated water until no chloride could be detected in the wash-water, filtered and rinsed by warm distilled water several times until the pH value was 6–7. The washed sample was dried at 110 °C. The yields of activated carbons were calculated according to the following equation:

$$\text{Yield of AC (wt\%)} = \frac{\text{Weight of activated carbon}}{\text{Weight of orange peel}} \times 100 \quad (1)$$

### 2.2. Characterization of adsorbent

The physical, structural and chemical properties of the activated carbon were determined by several analysis methods. The surface properties and surface area of the samples were characterized by $N_2$ adsorption measurements at 77 K using a surface area analyzer (TriStar 3000). The surface area ($S_{BET}$) was calculated from isotherms using the Brunauer–Emmett–Teller (BET) equation. The volume of liquid nitrogen corresponding to the amount adsorbed at a relative pressure of $P/P_0 = 0.99$ was defined as total pore volume (VT) [39]. The micropore volume ($V_\mu$) was determined from Dubinin–Radushkevich equation [40] and mesopore volume was calculated from the difference between $V_T$ and $V_\mu$. The pore diameter was calculated using the ratio 4 VT/SBET, and pore size distribution using the DFT method.

Fourier transforms infrared (FT-IR) spectroscopy analyses were performed using a spectrometer Perkin Elmer 283. The samples for FT-IR analyses were prepared by mixing them with KBr powder and pressing the mixture into pellets. The FT-IR spectra were recorded between 4000 and 400 $cm^{-1}$ (resolution of 4 $cm^{-1}$ and acquisition rate of 20 scan $min^{-1}$).

Ultimate analysis of the carbons was carried out in a C H N S Analyzer (LECO 932). Prior to analysis, the samples were dried overnight at 105 °C and cooled in desiccators. Oxygen content was obtained by the difference between the total percentage (100 wt.%) and the sum of percentages (wt.% dry ash free) of nitrogen, carbon, hydrogen and sulfur.

Ash content determination was done according to the ASTM D2866-94 method. Dry AC sample (1.0 g) was placed into a porcelain crucible and transferred into a preheated muffle furnace set at a temperature of 1000 °C. The furnace was left on for one hour after which the crucible and its content was transferred to desiccators and allowed to cool. The crucible and content was reweighed and the weight lost was recorded as the ash content of the AC sample. Then the % ash content (dry basis) was calculated from Eq. (1).

$$\text{Ash } \% = \frac{W_{ash}}{W_0} \times 100 \quad (2)$$

where $w_0$ is the dry weight of activated carbon sample before ashing.

In order to plot TGA (10 mg activated carbon, 10 °C/min, 10 ml/min $N_2$ flow rate) and DTA (10 mg activated carbon, 10 °C/min, 10 ml/min $O_2$ flow rate), curves for adsorbents, (Shimadzu DTA-50 TG/DTA thermal gravimetric analyzer) and losses in its mass were recorded. Heating procedures were started at room temperature and reached up to 800 °C by gradually increasing the temperature. The heating process is allowed to continue at this temperature for awhile; when no change in mass observed, the process is terminated.TGA and DTA graphs were plotted as a function of changes versus time and then construed.

SEM (Zeiss EVO 50 Model) was carried out to show the pore structure of obtained activated carbons. The SEM images were taken in secondary electrons; the acceleration voltage was equal to 20 kV, and the emission current was 20 pA.

The structures of these samples were checked by the powder XRD technology with Cu Kα radiation at room temperature, using a Rigaku diffractometer (MXP-AHP18) for 2Θ = 2–60°.

To specify MB numbers (Methylene blue number), 0.02 g of adsorbent was agitated with 10 mL 1000 mg $L^{-1}$ MB solutions for 12 h. Then, the mixture was filtrated through 0.45 μm nitrocellulose membrane. MB concentration left in the filtrate was determined by carrying out measurements in UV vis spectrophotometer (Shimadzu 2100S) at 668 nm [31]. Iodine numbers of adsorbent was defined according to ASTM D4607-94(1999) [32].

**Table 1**
Characteristics of the orange peel.

| Characteristics | Methods | Orange peels |
|---|---|---|
| Moisture content (wt.%) | ASTM D 2016 | 9.20 |
| *Proximate analysis (wt.%)* | | |
| Volatile matter | ASTM E 872 | 76.52 |
| Ash | ASTM D1102 | 3.09 |
| Fixed carbon | By difference | 20.39 |
| *Ultimate analysis (wt.%)* | LECO 932 Instrument | |
| Carbon | | 46.63 |
| Hydrogen | | 6.04 |
| Nitrogen | | 0.23 |
| Sulfur | | 0.05 |
| Oxygen | By difference | 47.05 |
| *Surface properties* | TriStar 3000 Instrument | |
| BET surface area ($m^2$ $g^{-1}$) | | 1 |
| Total pore volume ($cm^3$ $g^{-1}$) | | 0.001 |
| Mesopore volume ($cm^3$ $g^{-1}$) | | 5.67 |
| Micropore volume ($cm^3$ $g^{-1}$) | | n.d |

n.d.: not detection.

## 3. Results and discussion

### 3.1. Characterization results

#### 3.1.1. Ultimate analysis

Ultimate analysis results are given in Table 2. Results indicate that the carbonization temperatures influenced the yields of the activated carbons. An increase in the temperature a t the same concentrations for both $K_2CO_3$ and $ZnCl_2$ led to a decrease in the yields of the activated carbons. These findings show that both $K_2CO_3$ and

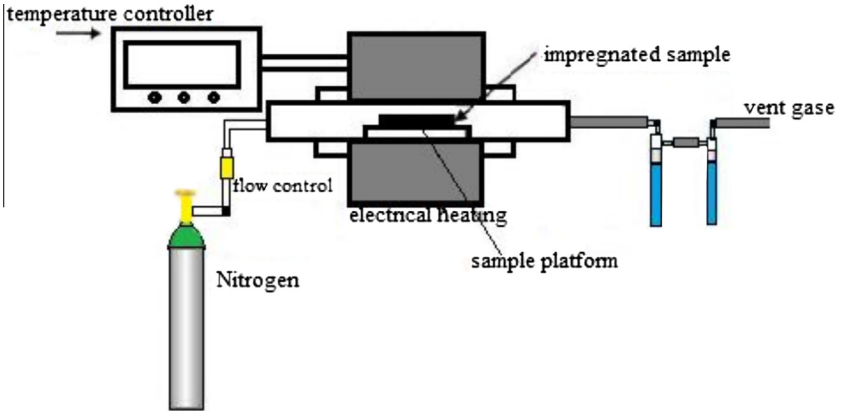


**Fig. 1.** Experimental setup.

**Table 2**
Product yields and ultimate analysis of activated carbons produced from $K_2CO_3$ and $ZnCl_2$ activation.

| Reagent | Activation temperature (°C) | Yield of AC (%wt)[c] | Ash | Ultimate analysis | | | | |
|---|---|---|---|---|---|---|---|---|
| | | | | C | H | N | O[a] | C/H[b] |
| $K_2CO_3$ | 500 | 22 | 7.09 | 77.97 | 2.85 | – | 19.45 | 2.28 |
| | 700 | 20 | 7.72 | 80.89 | 1.91 | – | 17.20 | 3.52 |
| | 800 | 18 | 8.80 | 77.69 | 1.67 | – | 20.64 | 3.87 |
| | 850 | 16 | 10.80 | 72.04 | 1.03 | – | 26.93 | 5.82 |
| | 900 | 17 | 10.34 | 72.01 | 1.07 | – | 26.92 | 5.61 |
| | 950 | 11 | 14.46 | 70.49 | 0.81 | – | 28.70 | 7.25 |
| | 1000 | 10 | 11.70 | 53.41 | 0.33 | – | 46.26 | 13.5 |
| $ZnCl_2$ | 400 | 40 | 0.26 | 79.27 | 2.97 | 1.17 | 16.59 | 2.22 |
| | 500 | 37 | 0.32 | 69.16 | 2.45 | 0.67 | 27.72 | 2.35 |
| | 600 | 35 | 0.35 | 63.90 | 1.76 | – | 34.34 | 3.03 |
| | 700 | 33 | 0.40 | 78.12 | 1.38 | 0.30 | 20.20 | 4.72 |
| | 800 | 32 | 0.47 | 79.16 | 0.97 | – | 19.87 | 6.80 |
| | 1000 | 31 | 2.54 | 84.06 | 0.87 | 0.67 | 14.40 | 8.05 |

[a] Calculated by difference.
[b] Mole ratio.
[c] Carbonization yield.

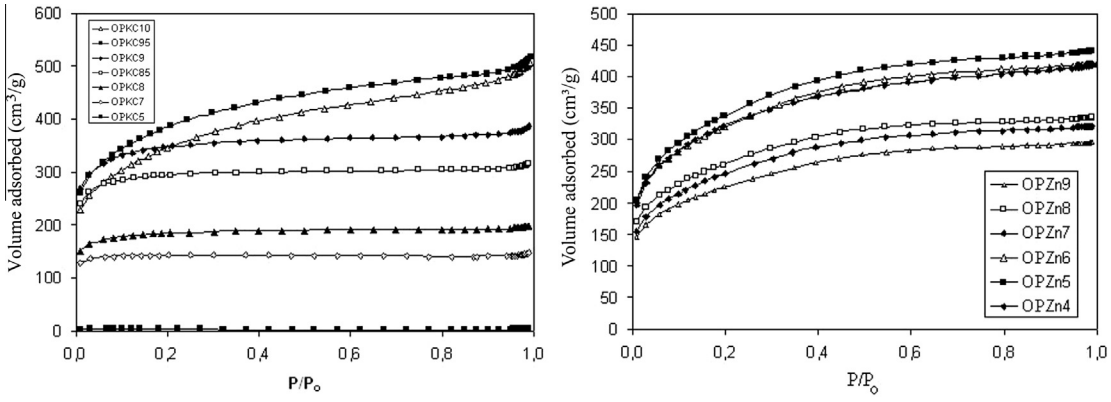


**Fig. 2.** Adsorption isotherms of $N_2$ at 77 K for (a) OPKC and (b) OPZn activated carbons.

$ZnCl_2$ worked efficaciously as activating reagents. Many reactions such as dehydration and elimination occur during carbonization due the release of low molecular compounds via cracking of chemical bonds in the lignocellulosic network with the help $K_2CO_3$ and $ZnCl_2$. The productions of activated carbons obtained by activation of $ZnCl_2$ almost have the same yield. However, $ZnCl_2$, a Lewis acid, contributes to aromatization of the structure as having only a dehydrating agent role in producing of AC. $ZnCl_2$ does not react with carbon; hence resultant yield is much higher compared to activated carbons obtained by $K_2CO_3$ activation [41]. Carbon atoms play a major role in the organized structure and aromatization. OPZ9 has the highest C content in all ACs, so the ratio of C/H has also increased by rising C percentage. An increment in the ratio of C/H indicates an increase of aromatization in the structure, hence formation of a regular structure as well as an increase in graphitization. $K_2CO_3$ react with carbon, hence resultant yield is much lower compared to activated carbons obtained by $ZnCl_2$ activation. There was no regular trend in oxygen contents of the

**Table 3**
Characteristics of activated carbons produced from $K_2CO_3$ and $ZnCl_2$ activation.

| Reagent | Activation temp. (°C) | $S_{BET}$ ($m^2$/g) | $S_{micro}$ ($m^2$/g) | $S_{ext}$ ($m^2$/g) | $V_{total}$ ($cm^3$/g) | $V_{micro}$ ($cm^3$/g) | $V_{mezo}$ ($cm^3$/g) | dp[a] (nm) |
|---|---|---|---|---|---|---|---|---|
| $K_2CO_3$ | 500 | 9 | 6 | 3 | 0.01 | 0.01 | 0.00 | 2.6 |
| | 700 | 477 | 442 | 35 | 0.23 | 0.21 | 0.02 | 1.8 |
| | 800 | 621 | 479 | 141 | 0.30 | 0.22 | 0.08 | 1.9 |
| | 850 | 987 | 798 | 190 | 0.48 | 0.37 | 0.11 | 1.9 |
| | 900 | 1177 | 864 | 313 | 0.59 | 0.40 | 0.19 | 2.0 |
| | 950 | 1352 | 505 | 847 | 0.79 | 0.22 | 0.57 | 2.3 |
| | 1000 | 1228 | 365 | 864 | 0.78 | 0.16 | 0.62 | 2.5 |
| $ZnCl_2$ | 400 | 1151 | 376 | 775 | 0.65 | 0.16 | 0.49 | 2.2 |
| | 500 | 1215 | 327 | 888 | 0.68 | 0.13 | 0.55 | 2.2 |
| | 600 | 1144 | 306 | 839 | 0.65 | 0.13 | 0.52 | 2.3 |
| | 700 | 882 | 213 | 669 | 0.50 | 0.09 | 0.41 | 2.3 |
| | 800 | 836 | 275 | 660 | 0.52 | 0.12 | 0.40 | 2.3 |
| | 1000 | 804 | 231 | 573 | 0.46 | 0.10 | 0.36 | 2.3 |

*S*: Surface area, *V*: pore volume and dp: average pore diameter.
[a] 4V/A by BET.

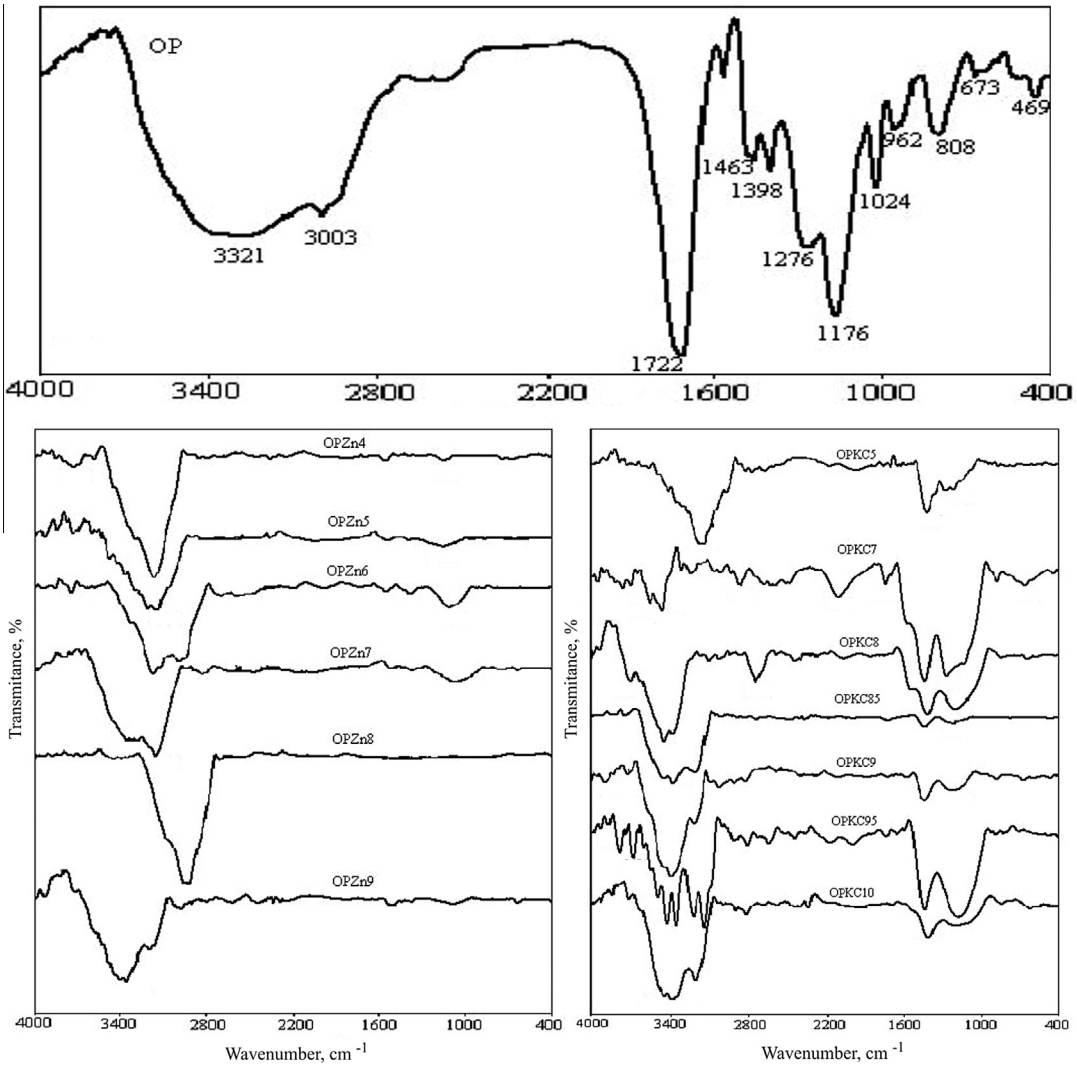


**Fig. 3.** FT-IR spectra of OPZn and OPKC activated carbons and raw material OP.

activated carbons produced from $K_2CO_3$ and $ZnCl_2$ while the carbon contents changed regularly. Carbon yields abated when the activation temperature was raised. Activated carbons from $K_2CO_3$ activation yielded lower product yields than those from $ZnCl_2$ activation. The ash contents of the activated carbons obtained from $K_2CO_3$ activation were higher than those of with $ZnCl_2$

*3.1.2. BET surface areas and pore sizes distribution*

In the chemical activation, the final activation temperature is important process parameters in determining the surface area and the pore volume of the activated carbon. Fig. 2 shows the $N_2$ adsorption isotherms and pore size distribution for OPKC and OPZn series. The effects of activation temperature on the surface

areas (BET) and pore volume (micropore and mesopore) and pore volumes (total, micropore, and mesopore) of the activated carbons are shown in Table 3. When the activation temperature increased from 400 to 500 °C and from 500 to 950 °C the $S_{BET}$ and $V_{total}$ values increased significantly and $S_{BET}$ reached 1215 $m^2/g$ and 1352 $m^2/g$, for $ZnCl_2$ and $K_2CO_3$ activation, respectively. However, at high temperatures the trend was reversed due to the sintering effect of the volatiles and the shrinkage of the carbon structure, resulting in the narrowing and closing up to some of the pores.

*3.1.3. FT-IR analysis*

The FT-IR spectrum of OP, OPZn and OPKC activated carbons are shown in Fig. 3. The spectra display a number of adsorption peaks, indicating the complex nature of the material examined. OP, which was not subjected to heat treatment and hence, contains especially volatile compounds, is the richest in terms of functional groups compared to other adsorbents. The broad and intense absorption peaks in the 3700–3100 $cm^{-1}$ correspond to the O—H stretching vibrations of cellulose, pectin, absorbed water, hemicellulose, and lignin [42]. The peaks observed at 3003 $cm^{-1}$ can be attributed to the aliphatic saturated C—H stretching vibrations of in lignin polysaccharides including cellulose and hemicelluloses [43]. The presence of the peak at 1722 $cm^{-1}$ in the OP spectrum indicates the carbonyl (C=O) stretching vibration of the carboxyl groups of pectin, hemicellulose and lignin in the OP [21]. The weak peaks around 1600 cm−1 are due to the C=C stretching that can be attributed to the presence of aromatic or benzene rings in lignin. The vibrations at 1463–1398 $cm^{-1}$ could be due to aliphatic and aromatic (C—H) groups in the plane deformation vibrations of methyl, methylene and methoxy groups. The bands in the range of 1300–1000 $cm^{-1}$ can be assigned to the C—O stretching vibration of carboxylic acids and alcohols [44]. The region in between 700 and 900 $cm^{-1}$ contains various bands related to aromatic, out of plane C—H bending with different degrees of substitution [45]. Some similarities for all investigated samples were observed when the FTIR spectrum for the OPZn and OPKC activated carbons are compared to that for raw material (OP). Where a broad region of absorption involving overlapping bands in the range 3700–3100 $cm^{-1}$ existed but slightly shifted from sample to another in the location and intensity. This region includes the bands assigned to OH and CH in aromatic system stretching vibrations. This finding is apparently due to the fact that activated reagent initiated bond cleavage, leading to dehydration and elimination reactions that release volatile products such as water, acetic acid, methanol and furan derivatives [29,30]. This is followed by partial aromaticity and re-combination of species to form a stronger cross-linked solid. In other words, the many bonds are broken in aliphatic and aromatic species present in the precursor material leading to liberation and elimination of many light and volatile substrates causing partial aromatization and thus carbonization. This behavior is also consistent with the disappearance of C=O at 1722 $cm^{-1}$ in the OPZn and OPKC spectrum. The broad bands

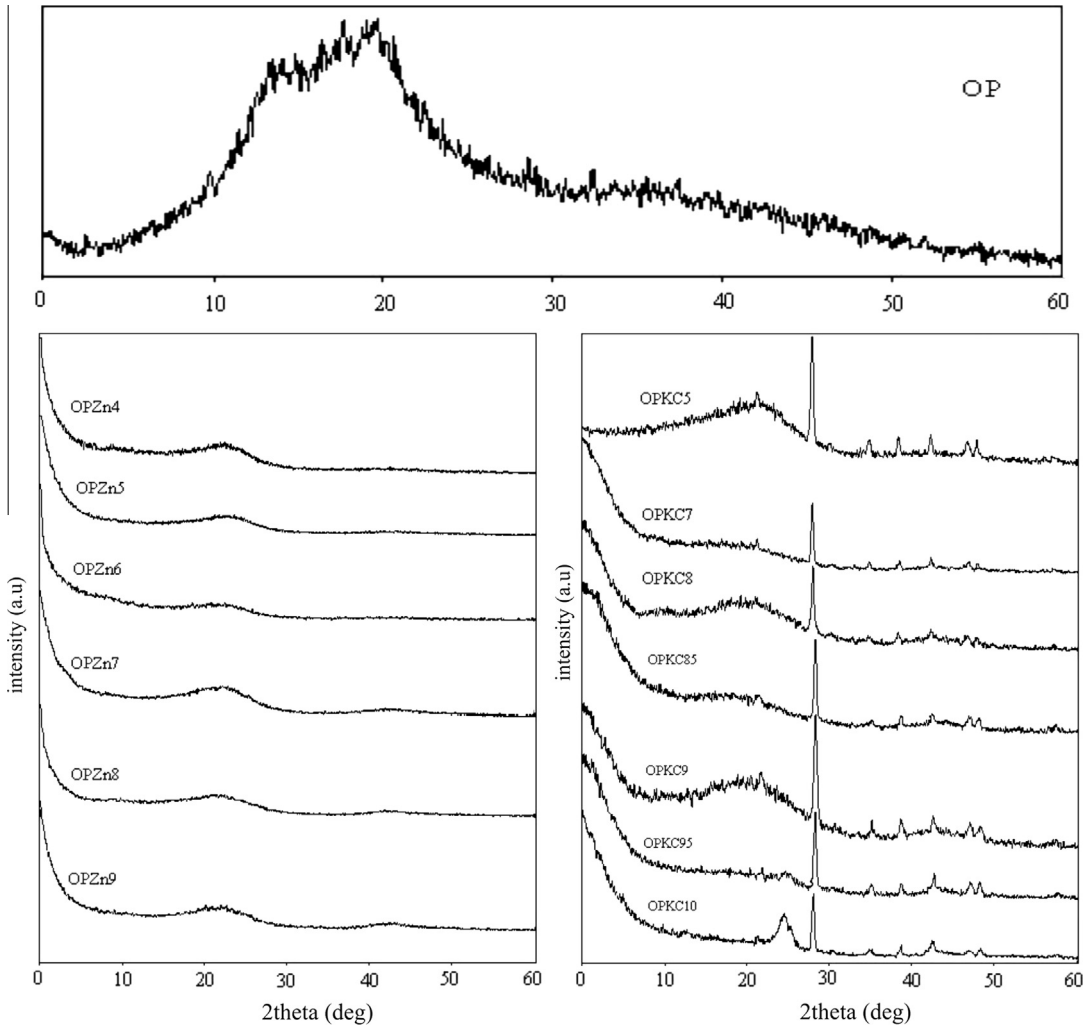


**Fig. 4.** XRD spectra of produced activated carbons and raw material.

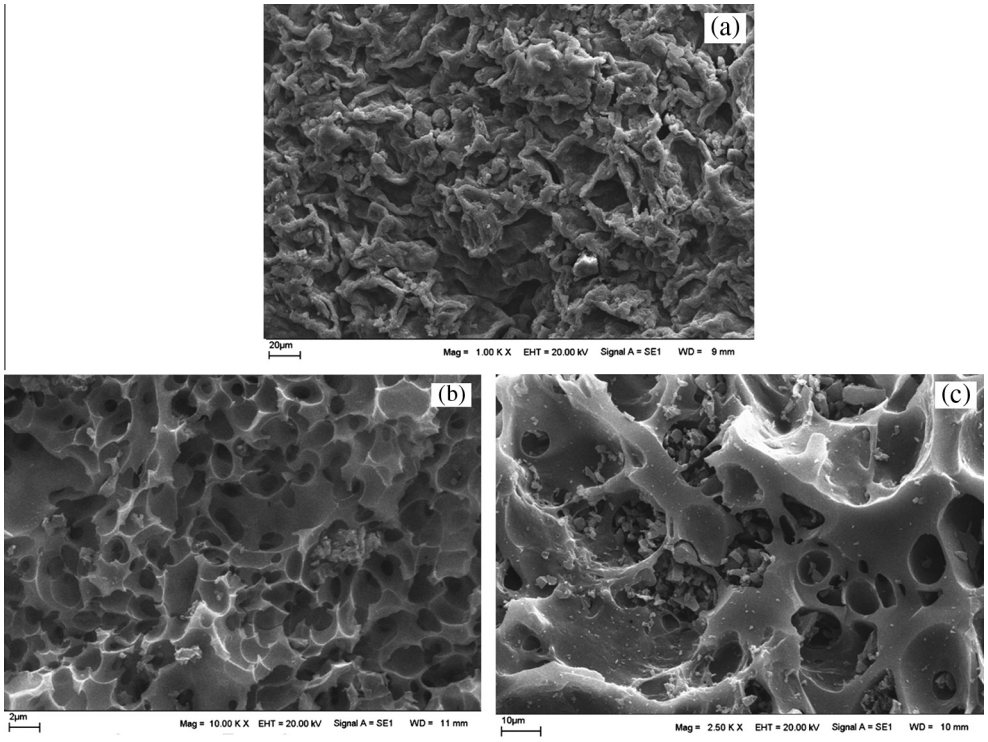


**Fig. 5.** SEM micrographs of (a) OP (b) OPKC95 and (c) OPZn5.

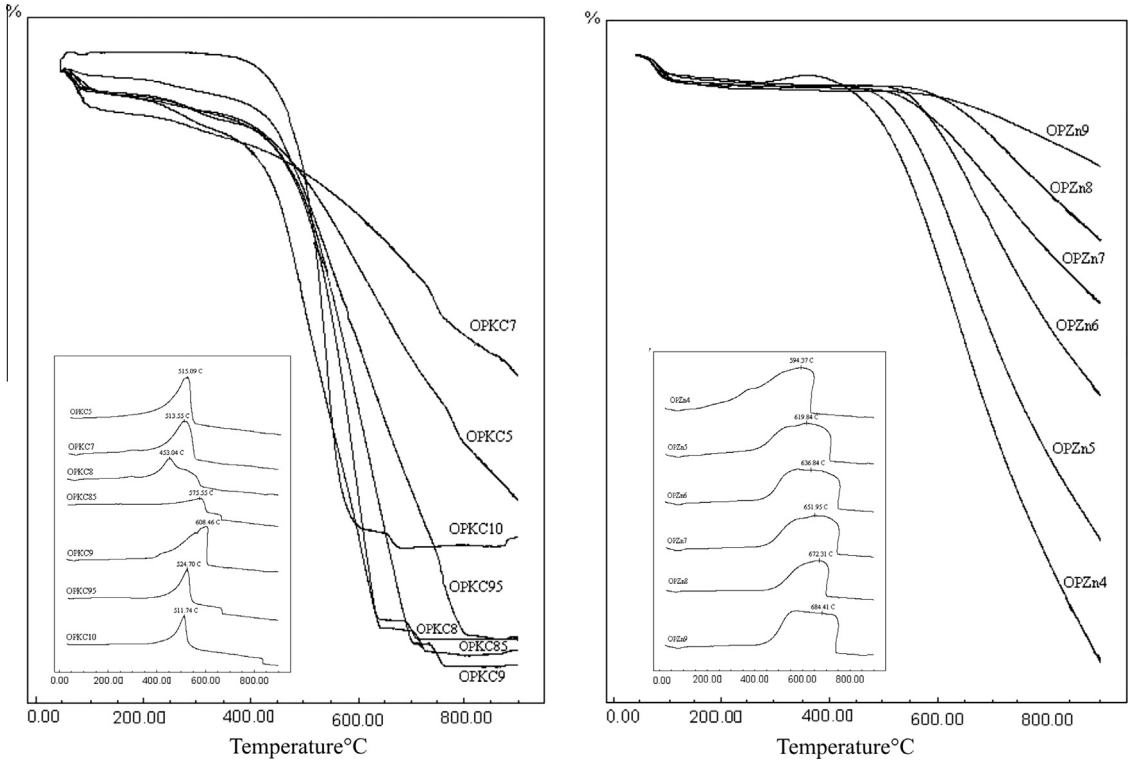


**Fig. 6.** TGA and DTA analyses of activated carbons.

1000–1300 $cm^{-1}$ has been assigned to C—O stretching in acids, alcohols, phenols, ethers and esters. The bands disappeared for the OPZn. This obviously indicates that C—O bonds in acids, alcohols, phenols, ethers and esters are vanished during activation processes. The weak band appears at ~1600 in the OPZn spectrum is consistent with aromatization. For FTIR spectra of OPKC activated carbons without HCl washing, the overlapping bands in the range 1500–1000 $cm^{-1}$ are attributed to carbonyl group, carboxylate ion, ash composition and chelat bounded carboxylate structure. These carbonyl group and carboxylate functional group are formed

possibly due to the oxidative degradation of aromatic ring during the $K_2CO_3$ impregnation and heat treatment stages. In the OPZn spectrum, the disappearances of carbonyl and carboxylate ion groups were due to hydrolysis effect of the HCl.

*3.1.4. XRD analysis*

The X-ray diffraction profile of the raw (OP) and activated carbon materials (OPZn and OPKC) are shown in Fig. 4. The X-ray diffraction spectrum did not exhibit well-defined peaks in any region, which indicated that no discrete mineral phase was detected. Thus, the orange peel has a completely amorphous structure, which is expected for organic materials. The hump in the 2Θ range 20–30° implies the high degree of disorder expected for the produced carbonaceous material. This character is maintained in case of the activating agents $ZnCl_2$ and $K_2CO_3$. The pattern of the OPZn sample showed no defined peaks related to any crystalline phase. In case of the $K_2CO_3$, patterns displayed defined and considerably sharp peaks due to the corresponding $K_2CO_3$. The formation of such crystalline phases has apparently induced the formation of an ordered carbon texture as inferred from the appearance, in these cases, of peaks due to graphite.

As OPZn and OPKC samples have been subjected to the different protocol of washing and the different situation in case of $K_2CO_3$ could be attributed to the strong mode of interaction with carbon matrix that caused some of the remaining part of the activating agent to escape the complete removal with a consequent formation of the oxidic phase upon thermal treatment. The XRD patterns of OPKC series show the two typical bands of carbon materials and some extra sharp peaks associated to the presence of heteroatoms due to inorganic oxides in the ACs.

*3.1.5. SEM analysis of the adsorbents*

Scanning electron microscopy (SEM) technique was used to investigate the surface physical morphology of activated carbons. Fig. 5 illustrates the SEM photographs of orange peel and activated carbons produced at different activation temperatures (OPZn5 and OPKC95). It can be seen there was channel-like wall on the surface of raw material. After activation, the thick wall got opened and the surface turned into smooth with many different sizes and shapes cavities. OPKC95 exhibited honeycomb-like pores. The SEM images of OPZn5 showed an irregular and heterogeneous surface morphology with a well-developed porous structure. It can be seen from the micrographs that the external surface of the activated carbons has cracks, crevices, and some grains in various sizes in large holes. Pores of different sizes shapes could be observed.

*3.1.6. TGA and DTA analyses*

The thermal stability of the carbon materials were analyzed by TG-DTA and are depicted in Fig. 6. During the thermo gravimetric analysis (TGA) weight loss stages were observed in all activated carbons. All AC samples are generally similar to each other, but start and end-point of the peaks shift to higher values with increasing temperature. The peak located between 400 and 600 °C is present in AC samples. Weight loss value of OPKC series are between 32 and 81 wt%. The lowest total mass loss produced to 700 °C (OPKC7) is 32 wt%, the highest total mass loss produced to 900 °C is 81 wt%. Weight loss value of OPZn series are between 10 and 72 wt%. The orange peel commonly consists of cellulose, hemi-cellulose and lignin. Cellulose decomposes in the temperature ranges of 573–703 °C. Hemi-cellulose decomposes at much lower temperature. Among the three components, lignin was the most difficult one to decompose. Its decomposition happened slowly under the whole temperature range from ambient to 900 °C [46,47].

Therefore, the peak of the weight loss rate around 600 K corresponds to the decomposition of cellulose and the long tail between 700 and 900 K corresponds to the decomposition of lignin. Two peaks of the rate are observed around 600 K for the OPKC. The first peak and the second peak correspond to the decomposition of hemi-cellulose and that of cellulose, respectively. For the OPZn, the peak of the cellulose overlaps with that of the hemi-cellulose and therefore only a single peak appears in the weight loss rate [48].

*3.1.7. Iodine and methylene blue adsorption*

Methylene blue adsorption studies are widely used for the evaluation of adsorbents because this dye can be viewed as a model for visible pollution and is an indicator of mesoporosity. The capacity of adsorbents for removing color can be evaluated through iodine adsorption from aqueous solutions using test conditions referred to as iodine number determination. This indicates their relative activation level and the surface area available for micropores. The best conditions to prepare activated carbon from orange peel are chosen as OPKC95 and OPZn5 samples. İodine adsorption is 1564, 1396 mg/g for OPKC95 and OPZn5, respectively and methylene blue number of two samples obtained at these conditions is 150 mg/g. These values are compared with those of carbons prepared from different agricultural wastes (literature values are between 800 and 1200 mg/g) [49]. The high iodine number revealed that orange peel is efficient precursors for preparation of carbon with high micropores content.

## 4. Conclusion

Orange peel can be good precursors for producing highly porous activated carbon by simple preparative methods. Depending on the nature of the raw precursors, the treatment conditions and the activating agent, various types of activated carbons can be obtained. The main conclusion of the work now reported is that we were able to produce activated carbons from orange peel by chemical activation with $K_2CO_3$ and $ZnCl_2$ with good physical and chemical properties, in terms of adsorption properties, physical resistance and surface chemistry. The materials have shown good surface characteristics with a well developed microporous structure. According to the experimental results, activation with different chemical agents and temperatures strongly affects characteristics of the activated carbons and optimum activation temperature should be investigated in detail (between 900 and 950 °C for $K_2CO_3$, 400 and 500 °C for $ZnCl_2$ activation) to produce higher surface area and pore volume.

The main conclusions are as follows:

- The samples with higher burn-offs presented higher apparent BET surface area, for the $K_2CO_3$ series the values were between 9 and 1352 $m^2\ g^{-1}$ and micropore volume, by the αs method, between 0.01 and 0.79 $cm^3\ g^{-1}$. $ZnCl_2$ series results were a little lower with BET surface area between 804 and 1215 $m^2\ g^{-1}$, and micropore volume within the range 0.10–0.16 $cm^3\ g^{-1}$.
- Low yields of activated carbons were obtained by chemical activation. The yields of activated carbons were decreased with the increasing the activation temperature in the range of 40–31% for $ZnCl_2$ impregnation, 22–10% for $K_2CO_3$ impregnation.
- SEM images showed that pores of different size and different shapes were obtained from different chemical activation agents. $K_2CO_3$ impregnated sample forms honeycomb-like morphology; $ZnCl_2$ impregnated samples forms irregular and heterogeneous surface morphology with a well-developed porous structure after activation.
- $K_2CO_3$ was found more effective than the $ZnCl_2$ as a chemical reagent in terms of high surface area, porosity development, and surface morphology of the activated carbons. Depending

on the activation temperature and chemical reagents the surfaces of the activated carbons had the pores which were different sizes and shapes.

- The XRD patterns showed a predominantly amorphous structure of the activated carbon prepared, transforming it into a structure of greater crystalline at higher temperatures. The FTIR spectrum showed the presence of different oxygen groups and olefinic and aromatic carbon structures in the raw shell. Subsequent heat treatment resulted in the aromatization of the carbon structure and a decrease in the oxygen groups.

The production of activated carbons with high surface area from orange peel, a waste of fruit juice industries, is indeed of importance from the view point of economic and environmental aspects.

## References


[1] M.J. Martin, A. Artola, M.D. Balaguer, M. Rigola, Activated carbons developed from surplus sewage sludge for the removal of dyes from dilute aqueous solutions, Chem. Eng. J. 94 (2003) 231–239.

[2] R. Malik, D.S. Ramteke, S.R. Wate, Adsorption of malachite green on groundnut shell waste based powdered activated carbon, Waste Manage. 27 (9) (2007) 1129–1138.

[3] K. Kadirvelu, C. Namasivayam, Activated carbon from coconut coir pith as metal adsorbent: adsorption of Cd (II) from aqueous solution, Adv. Environ. Res. 7 (2003) 471–478.

[4] D. Prahas, Y. Kartika, N. Indraswati, S. Ismadji, Activated carbon from jackfruit peel waste by $H_3PO_4$ chemical activation: pore structure and surface chemistry characterization, Chem. Eng. J. 140 (2008) 32–42.

[5] O. Ioannidou, A. Zabaniotou, Agricultural residues as precursors for activated carbon production, Renew. Sustain. Energy Rev. 11 (2007) 1966–2005.

[6] W.T. Tsai, C.Y. Chang, S.L. Lee, Preparation and characterization of activated carbons from corn cob, Carbon 35 (1997) 1198–1200.

[7] Z. Hu, M.P. Srinivasan, Preparation of high-surface-area activated carbons from coconut shell, Micropor. Mesopor. Mater. 27 (1999) 11–18.

[8] W.M.A.W. Daud, W.S.W. Ali, M.Z. Suleiman, The effects of carbonization temperature on pore development in palm-shell-based activated carbon, Carbon 38 (2000) 1925–1932.

[9] F. Suárez-García, A. Martínez-Alonso, J.M.D. Tascon, Pyrolysis of apple pulp: chemical activation with phosphoric acid, J. Anal. Appl. Pyrol. 63 (2002) 283–301.

[10] J. Hayashi, A. Kazehaya, K. Muroyama, A.P. Watkinson, Preparation of activated carbon from lignin by chemical activation, Carbon 38 (2000) 1873–1878.

[11] Y. Diao, W.P. Walawender, L.P. Fan, Activated carbons prepared from phosphoric acid activation of grain sorghum, Bioresour. Technol. 81 (2002) 45–52.

[12] A.C. Lua, T. Yang, J. Guo, Effects of pyrolysis conditions on the properties of activated carbons prepared from pistachio-nut shells, J. Anal. Appl. Pyrol. 72 (2004) 279–287.

[13] S. Senthilkumaar, P.R. Varadarajan, K. Porkodi, C.V. Subbhuraam, Adsorption of methylene blue onto jute fiber carbon: kinetics and equilibrium studies, J. Colloid Interface Sci. 284 (2005) 78–82.

[14] J. Martinez, S. Norland, T.F. Thingstad, D.C. Schroeder, G. Bratbak, W.H. Wilson, A. Larsen, Variability in microbial population dynamics between similarly perturbed mesocosms, J. Plankton Res. 28 (2006) 783–791.

[15] M. Olivares-Marín, C. Fernández-González, A. Macías-Garcıa, V. Gómez-Serrano, M.A. Lillo-Rodensas, D. Carzrola-Ameros, A. Linares-Solano, Chemical reactions between carbons and NaOH and KOH – an insight into chemical activation mechanisms, Carbon 41 (2003) 265–267.

[16] B. Ash, D. Satapathy, P.S. Mukherjee, B. Nanda, J.L. Gumaste, B.K. Mishra, Characterization and application of activated carbon prepared from coir pith, J. Sci. Ind. Res. 65 (2006) 1008–1012.

[17] A. Gurses, C. Dogar, S. Karaca, M. Acikyildiz, R. Bayrak, Production of granular activated carbon from waste Rosa canina sp. seeds and its adsorption characteristics for dye, J. Hazard. Mater. B131 (2006) 254–259.

[18] R.M. Suzuki, A.D. Andrade, J.C. Sousa, M.C. Rollemberg, Preparation and characterization of activated carbon from rice bran, Bioresour. Technol. 98 (2007) 1985–1991.

[19] G. Ozgul, A. Ozcan, A.S. Ozcan, H.F. Gercel, Preparation of activated carbon from a renewable bio-plant of Euphorbia rigida by $H_2SO_4$ activation and its adsorption behavior in aqueous solutions, J. Appl. Surf. Sci. 253 (2007) 4843–4852.

[20] I.A.W. Tan, B.H. Hameed, A.L. Ahmad, Equilibrium and kinetic studies on basic dye adsorption by oil palm fibre activated carbon, Chem. Eng. J. 127 (2007) 111–119.

[21] B.H. Hameed, F.B.M. Daud, Adsorption studies of basic dye on activated carbon derived from agricultural waste: Hevea brasiliensis seed coat, J. Chem. Eng. 139 (2008) 48–55.

[22] H. Deng, L. Yangb, G. Taoa, J. Daia, Preparation and characterization of activated carbon from cotton stalk by microwave assisted chemical activation – application in methylene blue adsorption from aqueous solution, J. Hazard. Mater. 166 (2009) 1514–1521.

[23] Y.S. Ho, R. Malarvizhi, N. Sulochana, Equilibrium isotherm studies of methylene blue adsorption activated carbon prepared from Delonix regia pods, J. Environ. Prot. Sci. 3 (2009) 111–116.

[24] P. Sugumaran, S. Seshadri, Evaluation of selected biomass for charcoal production, J. Sci. Ind. Res. 68 (8) (2009) 719–723.

[25] P. Ravichandran, P. Sugumaran, S. Seshadri, Preparation and characterization of activated carbons derived from palmyra waste of coastal region, in: Proceedings of International Conference on "Impact of Climate Change on Coastal Ecosystem, India, 2011.

[26] S.K. Banerjee, M.D. Mathew, Carbonization of jute stick, Agro Waste 138 (1985) 217–227.

[27] T. Wigmans, Industrial aspects of production and use of activated carbon, Carbon 27 (1989) 13–22.

[28] K. Gergova, N. Petrov, S. Eser, Adsorption properties and microstructure of activated carbons produced from agricultural by-products by steam pyrolysis, Carbon 32 (1994) 693–702.

[29] S.J.T. Pollard, F.E. Thompson, G.L. McConnachie, Microporous carbons from Moringa oleifera husks for water purification in less developed countries, Water Res. 29 (1995) 337–347.

[30] C. Namasivayan, K. Kadirvelu, Activated carbons prepared from coir pith by physical and chemical activation methods, Bioresour. Technol. 62 (1997) 123–127.

[31] K. Kadirvelu, M. Palanival, R. Kalpana, S. Rajeshwari, Activated carbon from an agricultural by-product for the treatment of dyeing industry wastewater, Bioresour. Technol. 74 (2000) 263–265.

[32] M.A. Lillo-Rodensas, D. Carzrola-Ameros, A. Linares- Solano, Chemical reactions between carbons and NaOH and KOH – an insight into chemical activation mechanisms, Carbon 41 (2003) 265–267.

[33] G.G. Stavropoulos, A.A. Zabaniotou, Production and characterization of activated carbons from olive-seed waste residue, Micropor. Mesopor. Mater. 82 (2005) 79–85.

[34] Y. Guo, D.A. Rockstraw, Physical and chemical properties of carbons synthesized from xylan, cellulose, and Kraft lignin by $H_3PO_4$ activation, Carbon 44 (8) (2006) 1464–1475.

[35] N.H. Phan, S. Rio, C. Faur, L. Le Coq, P. Le Cloirec, T.H. Nguyen, Production of fibrous activated carbons from natural cellulose (jute, coconut) fibers for water treatment applications, Carbon 44 (2006) 269–277.

[36] T.H. Spreen, The Free Trade Area of the Americas and the Market for Processed Citrus Products Food and Agriculture Organization, China, 2001.

[37] K.Y. Foo, B.H. Hameed, Preparation, characterization and evaluation of adsorptive properties of orange peel based activated carbon via microwave induced $K_2CO_3$ activation, Bioresour. Technol. 104 (2012) 679–686.

[38] T.H. Spreen, The citrus industries of the United States and Mexico after Nafta, Rev. Chapingo Ser. Hortic. 6 (2000) 145–152.

[39] ASTM-D1762-84, Ann Book ASTM Stand. D1762-84, 1984, pp. 292–293.

[40] K.S.W. Sing, D.H. Everett, R.A.W. Haul, L. Moscou, R.A. Pierotti, J. Rouquérol, T. Siemienieswska, Reporting physisorption data for gas/solid systems with special reference to the determination of surface area and porosity, Pure Appl. Chem. 57 (1985) 603–619.

[41] A. Ahmadpour, D.D. Do, The preparation of activated carbon from macadamia nutshell by chemical activation, Carbon 35 (1997) 1723–1732.

[42] A. Gündoğdu, C. Duran, H.B. Sentürk, M. Soylak, M. İmamoğlu, Y. Onal, Physicochemical characteristics of a novel activated carbon produced from tea industry waste, Appl. Pyrol. 104 (2013) 249–259.

[43] H.D. Nguyen, T.T.T. Mai, N.B. Nguyen, T.D. Dang, M.L.P. Le, T.T. Dang, V.M. Tran, Novel method for preparing micro fibrilated cellulose from bamboo fibers, Nanosci. Nanotechnol. 4 (2013) 9–19.

[44] D. Angın, Production and characterization of activated carbon from sour cherry stones by zinc chloride, Fuel 115 (2013) 804–811.

[45] M. Mastalerz, R.M. Bustin, Application of reflectance micro-transform Infrared spectrometry in studying coal macerals, Fuel 74 (1995) 536–542.

[46] K. Raveebdran, A. Gauesh, C.K. Kartic, Pyrolysis characteristics of biomass and biomass component, Fuel 75 (8) (1996) 987–998.

[47] J.A. Caballero, A. Marcilla, J.A. Conesa, Thermogravimetric analysis of olive stones with sulphuric acid treatment, J. Anal. Appl. Pyrol. 4 (1997) 75–88.

[48] J. Katesa, S. Junpiromand, C. Tangsathitkulchai, Effect of carbonization temperature on properties of char and activated carbon from coconut shell, Suranaree J. Sci. Technol. 20 (4) (2013) 269–278.

[49] M.M. Saeed, M. Ahmed, A. Ghaffar, Adsorption profile of molecular iodine and iodine number of polyurethane foam, Separat. Sci. Technol. 38 (2003) 715–731.